

# Analytic two-loop master integrals for $tW$ production at hadron colliders: I

Long-Bin Chen<sup>1</sup>, Jian Wang<sup>2</sup>

<sup>1</sup>*School of physics and materials science, Guangzhou University, Guangzhou 510006, China*

<sup>2</sup>*School of Physics, Shandong University, Jinan, Shandong 250100, China*

## Abstract

We present the analytic calculation of two-loop master integrals that are relevant for  $tW$  production at hadron colliders. We focus on the integral families with only one massive propagator. After choosing a canonical basis, the differential equations for the master integrals can be transformed into the  $d\ln$  form. The boundaries are determined by simple direct integrations or regularity conditions at kinematic points without physical singularities. The analytical results in this work are expressed in terms of multiple polylogarithms, and have been checked with numerical computations.

# 1 Introduction

As the heaviest fundamental particle in the standard model (SM), the top quark has played a special role in testing the structure of the SM. It is also expected that the top quark has a close relation to new physics because its mass is around the scale of electroweak symmetry breaking. Precise measurement of its properties is an important task for experiments at the large hadron collider (LHC). The single top quark production can be used to detect the electroweak coupling of top quarks, especially to determine the Cabibbo-Kobayashi-Maskawa matrix element  $V_{tb}$ . Among the three channels, the  $tW$  associated production, of which the leading order Feynman diagrams are shown in Fig.1, has the second largest cross section at the LHC, making it experimentally measurable [1–7].

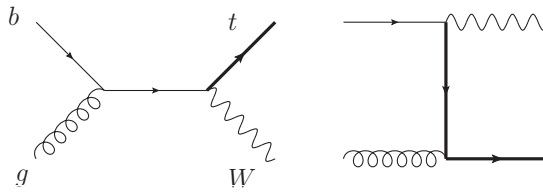


Figure 1: Leading order Feynman diagrams for  $gb \rightarrow tW$ .

In order to compare with the experimental results, precision theoretical predictions are indispensable. The fixed-order corrections have been computed only up to next-to-leading order in QCD for both the stable  $tW$  final state [8–11] or the process with their decays [12]. The parton shower and soft gluon resummation effects have been investigated in [13–15] and [16], respectively. Expanding the all-order formula of the threshold resummation to fixed orders, the approximate next-to-next-to-next-to-leading order total cross section has been obtained [17–20].

In the real corrections for  $tW^-$  production, there is a contribution from the  $gg(q\bar{q}) \rightarrow tW^- \bar{b}$  channel, which can interfere with the top quark pair production  $gg(q\bar{q}) \rightarrow t\bar{t}$  followed by the decay  $\bar{t} \rightarrow W^- \bar{b}$ . These resonance effects make the higher order correction so large that the perturbative expansion is no longer valid. There are several methods that have been proposed in the literature to deal with this problem. One can simply remove the Feynman diagrams containing two top quark resonances if the gauge dependence is negligible [13]. In a gauge invariant way, one could subtract the contribution of the  $t\bar{t}$  on-shell production and decay from the total  $tW(b)$  cross section either globally [9, 21] or locally [13, 14]. The interference can also be suppressed just by choosing special cuts on the final-state particles [12, 22–24] so that there is a clear definition of the  $tW$  production channel. See [25] for a review of these methods and implementation in MadGraph5\_aMC@NLO.

So far, the exact next-to-next-to-leading order QCD corrections are still unavailable, though the next-to-next-to-leading order N-jettiness soft function of this process, one of the ingredients for a full next-to-next-to-leading order differential calculation using a slicing method, has been calculated in [26, 27]. The main bottleneck is the two-loop virtual correction, which involves multiple scales. It is the purpose of this paper to start the first step toward tackling this problem.

The last a few decades have seen impressive progress of understanding the structure underlying the scattering amplitude and of the calculation of multi-loop Feynman integrals. For a specific process at a collider, the corresponding Feynman integrals can be categorized into different families according to their propagator configurations. And then the integrals in each family can be reduced to a small set of basis integrals, which are called master integrals, by making use of the algebraic relations among them, such as the identities generated via Integration by Parts (IBP) [28]. The number of master integrals has proven to be finite [29]. This IBP reduction procedure has been implemented in public computer programs, such as AIR [30], Reduze [31], LiteRed [32], FIRE [33], Kira [34], based on the Laporta algorithm [35]. As a consequence, the main task is to evaluate the master integrals either analytically or numerically; see recent reviews [36, 37]. For multi-loop integrals with multiple scales, it turns out that the differential equation is an efficient analytic method [38, 39] since it avoids the direct loop integration, which is rather complicated in some cases, by transforming the problem to finding a solution of a set of partial differential equations. This method has become widely used in a lot of multi-loop calculations after the observation that the differential equations can significantly simplify after choosing a canonical basis [40].

The rest of this paper is organized as follows. In section 2, we present the canonical basis and the corresponding differential equations. We discuss the determination of boundary conditions and present the analytical results in section 3. The conclusion is given in section 4.

## 2 The canonical basis and differential equations

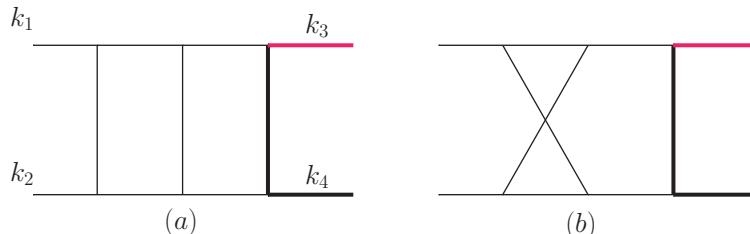


Figure 2: The planar (left) and non-planar (right) diagrams of the two-loop master integrals for  $gb \rightarrow Wt$  with one massive propagator. The massive external momenta are defined by  $k_3^2 = m_W^2, k_4^2 = m_t^2$  and we consider that  $k_1, k_2$  are ingoing while  $k_3, k_4$  are outgoing.

The process of  $g(k_1)b(k_2) \rightarrow W(k_3)t(k_4)$  contains two massive final states with different masses. For the external particles, there are on-shell conditions  $k_1^2 = 0, k_2^2 = 0, k_3^2 = m_W^2$  and  $k_4^2 = (k_1 + k_2 - k_3)^2 = m_t^2$ . The Mandelstam variables are defined as

$$s = (k_1 + k_2)^2, \quad t = (k_1 - k_3)^2, \quad u = (k_2 - k_3)^2 \quad (1)$$

with  $s + t + u = m_W^2 + m_t^2$ . For later convenience, we define dimensionless variables  $y$  and  $z$  as

$$t = y m_t^2, \quad m_W = z m_t. \quad (2)$$

It is usually believed that the more massive propagators a diagram involves, the more complicated the result is. The two-loop virtual corrections can have up to four massive propagators. Therefore, it is natural to divide the calculation to different parts according to the number of the massive propagators. In this paper, we focus firstly on the diagrams with a single massive propagator. Fig.2 shows two such diagrams with a double box topology, one being planar while the other non-planar. We discuss only the planar diagram in the main text, leaving the non-planar diagram to the appendix. The amplitude of the planar diagram has been reduced to ten form factors in [41].

We define the planar integral family, including the master integral shown in Fig.2(a), in the form of

$$I_{n_1, n_2, \dots, n_9} = \int \mathcal{D}^D q_1 \mathcal{D}^D q_2 \frac{1}{D_1^{n_1} D_2^{n_2} D_3^{n_3} D_4^{n_4} D_5^{n_5} D_6^{n_6} D_7^{n_7} D_8^{n_8} D_9^{n_9}}, \quad (3)$$

with

$$\mathcal{D}^D q_i = \frac{(m_t^2)^\epsilon}{i\pi^{D/2} e^{-\epsilon \gamma_E}} d^D q_i, \quad D = 4 - 2\epsilon. \quad (4)$$

The nine denominators are given by

$$\begin{aligned} D_1 &= q_1^2, & D_2 &= q_2^2, & D_3 &= (q_1 - k_1)^2, \\ D_4 &= (q_1 + k_2)^2, & D_5 &= (q_1 + q_2 - k_1)^2, \\ D_6 &= (q_2 - k_1 - k_2)^2, & D_7 &= (q_2 - k_3)^2 - m_t^2, \\ D_8 &= (q_1 + k_1 + k_2 - k_3)^2 - m_t^2, & D_9 &= (q_2 - k_1)^2. \end{aligned}$$

Because of momentum conservation, we do not need  $k_4$  in the denominators. The first seven denominators can be read directly from Fig.2(a). The last two are added to form a complete basis for all Lorentz scalars that can be constructed from two loop momenta and three independent external momenta. The denominators  $D_8, D_9$  appear only with non-negative powers. They take a form that is vanishing when the loop momentum,  $q_1$  or  $q_2$ , becomes soft, and therefore they are less divergent. Besides, the choice of  $D_9$  can be justified following the method in [42]. If we put the four massless propagators containing  $q_1$  on-shell, then we get a Jacobian

$$J = \frac{1}{(k_1 + k_2)^2 (q_2 - k_1)^2}. \quad (5)$$

From the one-loop calculation, we know the remaining three uncut propagators containing  $q_2$  already form a MI in  $\epsilon$ -form (up to a factor depending on the external momenta). Therefore, a  $D_9$  in the numerator would just cancel the hidden  $q_2$  propagator in the Jacobian.

Making use of the FIRE package, we find that the integrals in the planar family can be reduced to a basis of 31 MIs after considering the symmetries between integrals. We first select the MIs in such a form that the differential equations have coefficients linear in  $\epsilon$ . These MIs are given by

$$\begin{aligned} M_1 &= \epsilon^2 I_{0,0,0,1,2,0,2,0,0}, & M_2 &= \epsilon^2 I_{0,0,1,0,2,0,2,0,0}, & M_3 &= \epsilon^2 I_{0,0,2,0,2,0,1,0,0}, \\ M_4 &= \epsilon^2 I_{0,0,1,0,2,2,0,0,0}, & M_5 &= \epsilon^3 I_{0,0,1,0,2,1,1,0,0}, & M_6 &= \epsilon^2 I_{0,0,1,2,0,0,2,0,0}, \\ M_7 &= \epsilon^3 I_{0,0,1,1,1,0,2,0,0}, & M_8 &= \epsilon^2 I_{0,0,1,1,1,0,3,0,0}, & M_9 &= \epsilon^2 I_{0,0,2,1,1,0,2,0,0}, \\ M_{10} &= \epsilon^3 I_{0,1,0,1,2,0,1,0,0}, & M_{11} &= \epsilon^2 I_{0,1,0,1,2,0,2,0,0}, & M_{12} &= \epsilon^2 I_{0,1,1,2,0,0,2,0,0}, \end{aligned}$$

$$\begin{aligned}
M_{13} &= \epsilon^2 I_{0,1,1,2,0,2,0,0,0}, & M_{14} &= \epsilon^3 I_{0,1,1,2,0,1,1,0,0}, & M_{15} &= \epsilon^4 I_{0,1,1,1,1,0,1,0,0}, \\
M_{16} &= \epsilon^2 I_{1,0,0,0,2,0,2,0,0}, & M_{17} &= \epsilon^2 I_{2,0,0,0,2,0,1,0,0}, & M_{18} &= \epsilon^4 I_{1,0,1,0,1,1,1,0,0}, \\
M_{19} &= \epsilon^3 I_{1,0,1,0,1,1,2,0,0}, & M_{20} &= \epsilon^3 I_{1,0,1,1,1,0,2,0,0}, & M_{21} &= \epsilon^2 I_{1,0,1,1,1,0,3,0,0}, \\
M_{22} &= \epsilon^3 I_{1,1,0,0,2,0,1,0,0}, & M_{23} &= \epsilon^3 I_{1,1,0,0,2,1,0,0,0}, & M_{24} &= \epsilon^3 (1 - 2\epsilon) I_{1,1,0,0,1,1,1,0,0}, \\
M_{25} &= \epsilon^3 I_{1,1,0,0,2,1,1,0,0}, & M_{26} &= \epsilon^4 I_{1,1,0,1,1,0,1,0,0}, & M_{27} &= \epsilon^3 I_{1,1,0,1,1,0,2,0,0}, \\
M_{28} &= \epsilon^4 I_{1,1,1,1,1,0,1,0,0}, & M_{29} &= \epsilon^4 I_{1,1,1,1,1,1,1,0,0}, & M_{30} &= \epsilon^4 I_{1,1,1,1,1,1,1,0,-1}, \\
M_{31} &= \epsilon^4 I_{1,1,1,1,1,1,1,-1,0}.
\end{aligned} \tag{6}$$

The corresponding topology diagrams are displayed in Fig.3.

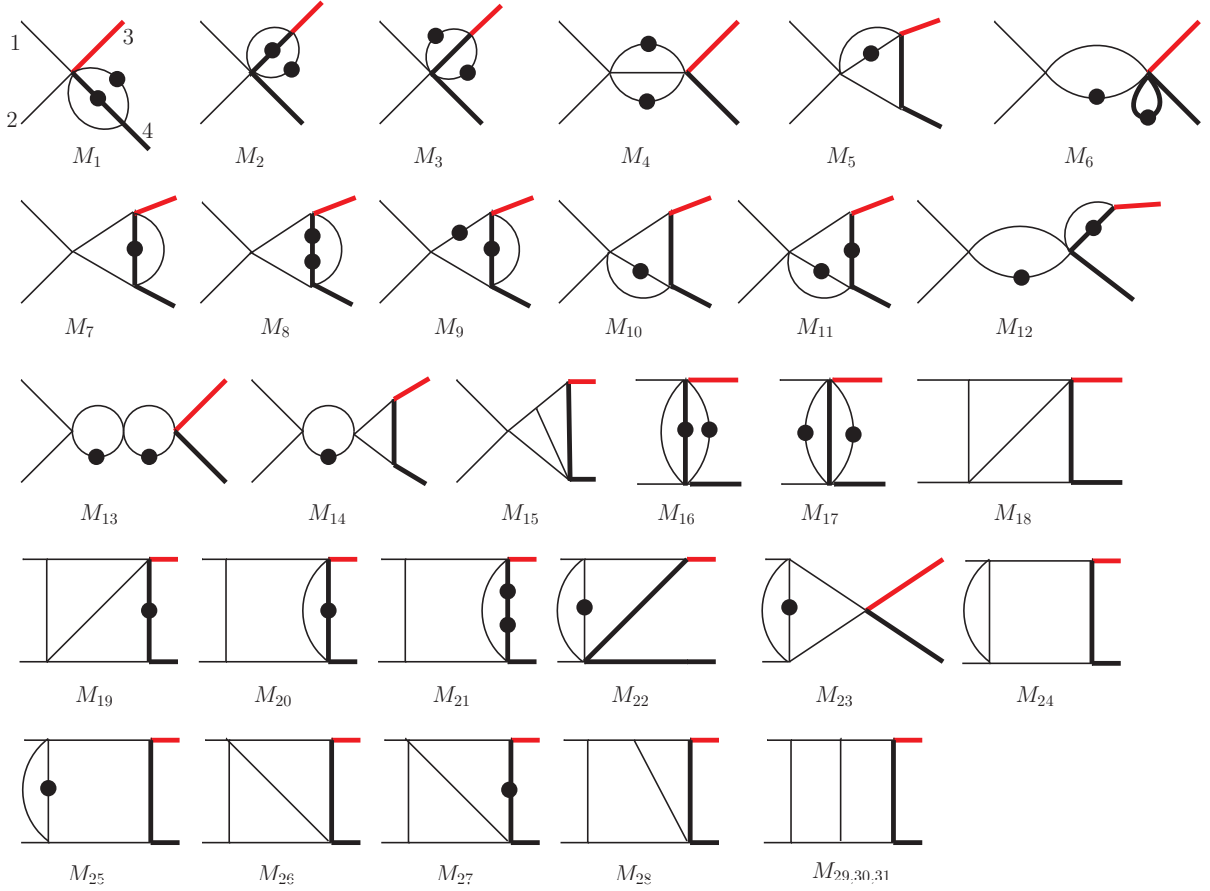


Figure 3: Master integrals in the planar family. The thin lines stand for massless particles while the thick lines for massive ones. The red line in the final state denotes  $W$ . Each block dot indicates one additional power of the corresponding propagator. Numerators are not shown explicitly in the diagram and could be found in the text.

Then we transform the MIs to a canonical basis using a method similar to that described in [43], starting from the lower sectors (with fewer propagators) to higher sectors (with more propagators). The main logic is to treat the  $\epsilon$  parts in the differential equations as perturbations. After solving the differential equation in four dimensions, i.e., omitting the perturbations, we get the dominant part of the MIs. Then the full solution can be obtained by using the method of variation of constants. The coefficient functions varied from the constants obey the canonical form of differential equations. For the integrals in the same sector, we have chosen a basis such that the differential equations vanishing in

four dimensional spacetime. For example,  $F_2$  and  $F_3$  belong to the same sector. They satisfy differential equations

$$\begin{aligned}\frac{dM_2}{dz} &= -\frac{2(1+\epsilon)}{z}M_2 - \frac{2\epsilon}{z}M_3, \\ \frac{dM_3}{dz} &= \left(\frac{4(1+\epsilon)}{z} - \frac{2(1+\epsilon)}{z-1} - \frac{2(1+\epsilon)}{z+1}\right)M_2 + \left(\frac{4\epsilon}{z} - \frac{1+4\epsilon}{z-1} - \frac{1+4\epsilon}{z+1}\right)M_3.\end{aligned}\quad (7)$$

Solving the above equations at  $\epsilon = 0$ , we find that the differential equations for the new basis

$$\begin{aligned}F_2 &= m_W^2 M_2, \\ F_3 &= (m_W^2 - m_t^2) M_3 - 2m_t^2 M_2\end{aligned}\quad (8)$$

are vanishing at  $\epsilon = 0$ . Going back to  $4 - 2\epsilon$  dimension, we have

$$\begin{aligned}\frac{dF_2}{dz} &= \epsilon \left( \frac{2F_2}{z} - \frac{2F_2 + F_3}{z-1} - \frac{2F_2 + F_3}{z+1} \right), \\ \frac{dF_3}{dz} &= \epsilon \left( \frac{8F_2}{z} - 2\frac{2F_2 + F_3}{z-1} - 2\frac{2F_2 + F_3}{z+1} \right).\end{aligned}\quad (9)$$

where the parameter  $\epsilon$  of the spacetime dimension appears only as a multiplicative factor on the right hand side of the differential equations, which is called the canonical form or the  $d\ln$  form [40].

In this way, we obtain the following MIs that obey canonical differential equations.

$$\begin{aligned}F_1 &= m_t^2 M_1, & F_2 &= m_W^2 M_2, & F_3 &= (m_W^2 - m_t^2) M_3 - 2m_t^2 M_2, \\ F_4 &= (-s) M_4, & F_5 &= r_1 M_5, & F_6 &= (-s) M_6, & F_7 &= r_1 M_7, \\ F_8 &= m_t^2 r_1 M_8, & F_9 &= m_W^2 s M_9 + m_t^2 (m_t^2 - m_W^2 - s) M_8 + \frac{3}{2}(m_t^2 - m_W^2 - s) M_7, \\ F_{10} &= r_1 M_{10}, & F_{11} &= m_t^2 (-s) M_{11} - \frac{3}{2}(m_t^2 - m_W^2 + s) M_{10}, \\ F_{12} &= m_W^2 s M_{12}, & F_{13} &= s^2 M_{13}, & F_{14} &= (-s) r_1 M_{14}, & F_{15} &= r_1 M_{15}, \\ F_{16} &= t M_{16}, & F_{17} &= (t - m_t^2) M_{17} - 2m_t^2 M_{16}, & F_{18} &= (m_W^2 - s - t) M_{18}, \\ F_{19} &= m_t^2 (-s) M_{19}, & F_{20} &= t (-s) M_{20}, & F_{21} &= m_t^2 (-s) ((t - m_t^2) M_{21} - M_{20}), \\ F_{22} &= (t - m_W^2) M_{22}, & F_{23} &= (-s) M_{23}, & F_{24} &= r_1 M_{24}, \\ F_{25} &= (t - m_t^2) (-s) M_{25}, & F_{26} &= (m_t^2 - s - t) M_{26}, \\ F_{27} &= -(m_W^2 t - m_t^2 (s + t + m_W^2) + m_t^4) M_{27}, \\ F_{28} &= (t - m_W^2) (-s) M_{28}, & F_{29} &= -(t - m_t^2) s^2 M_{29}, & F_{30} &= (-s) r_1 M_{30}, \\ F_{31} &= s^2 (M_{31} + M_{14}) + s \left( -M_{15} - M_{10} + 2M_7 - \frac{3}{2}M_5 + 3m_t^2 M_8 \right) \\ &+ (s + t - m_W^2) \left( s M_{25} - \frac{1}{4}M_{17} \right) - \frac{s + t - m_W^2}{4(t - m_t^2)} [2(m_t^2 + 2m_W^2) M_2 - 3s M_4 \\ &+ (m_t^2 - m_W^2) M_3 - 2(2t + m_t^2) M_{16} + 12(s + t - m_W^2) M_{18} + 8m_t^2 s M_{19}].\end{aligned}\quad (10)$$

The combination coefficients are generally just rational functions in  $s, t, m_W^2, m_t^2$ , except the square root product  $r_1 \equiv \sqrt{s - (m_t - m_W)^2} \sqrt{s - (m_t + m_W)^2}$  in the basis integrals such as  $F_5, F_7$ . This square root also appears in the differential equations. It is

necessary to first rationalize the square root before solving the differential equations in terms of multiple polylogarithms. To achieve this goal, we perform the following change of integration variable,

$$s = m_t^2 \frac{(x+z)(1+xz)}{x} \quad (11)$$

with  $-1 < x < 1$  so that  $r_1 = (1-x)(1+x)z/x$ . Notice that  $r_1$  is negative (positive) when  $s$  is negative (positive). Here we choose  $m_W$  or  $z$  also as a variable because it is easy to determine the boundary conditions for some integrals at  $z = 0$ . Then, the differential equations for  $\mathbf{F} = (F_1, \dots, F_{31})$  can be written as

$$d\mathbf{F}(x, y, z; \epsilon) = \epsilon (d\tilde{A}) \mathbf{F}(x, y, z; \epsilon), \quad (12)$$

with

$$d\tilde{A} = \sum_{i=1}^{15} R_i d\ln(l_i), \quad (13)$$

where  $R_i$  are rational matrices. Their explicit forms are provided in an auxiliary file. The arguments  $l_i$  of this  $d\ln$  form, which contain all the dependence of the differential equations on the kinematics, are referred to as the *alphabet* and they consist of the following letters,

$$\begin{aligned} l_1 &= x, & l_2 &= x+1, \\ l_3 &= x-1, & l_4 &= x+z, \\ l_5 &= xz+1, & l_6 &= xy+z, \\ l_7 &= xz+y, & l_8 &= y, \\ l_9 &= y-1, & l_{10} &= y-z^2, \\ l_{11} &= z, & l_{12} &= z^2-1, \\ l_{13} &= x^2z+xy+x+z, & l_{14} &= x^2z+x(y+z^2)+z, \\ l_{15} &= x^2z+x(-yz^2+y+2z^2)+z, & l_{16} &= x^2z+xy+z, \\ l_{17} &= x^2z^3+xy(z^2-1)+2xz^2+z^3. \end{aligned} \quad (14)$$

Notice that the last two letters,  $l_{16}$  and  $l_{17}$ , only appears for the non-planar integral family discussed in the appendix.

Since the roots of the letters above are purely algebraic, the solutions of the differential equations can be directly expressed in terms of multiple polylogarithms [44], which are defined as  $G(x) \equiv 1$  and

$$G_{a_1, a_2, \dots, a_n}(x) \equiv \int_0^x \frac{dt}{t - a_1} G_{a_2, \dots, a_n}(t), \quad (15)$$

$$G_{\vec{0}_n}(x) \equiv \frac{1}{n!} \ln^n x. \quad (16)$$

The length  $n$  of the vector  $(a_1, a_2, \dots, a_n)$  is referred to as the transcendental *weight* of multiple polylogarithms.

### 3 Boundary conditions and analytical results

In order to obtain the analytical solutions of the differential equations for the canonical basis shown above, we need to fix the boundary conditions first.

The base  $F_1$  is obtained by integration directly, which can also be found in [45].

$$F_1 = -\frac{1}{4} - \epsilon^2 \frac{5\pi^2}{24} - \epsilon^3 \frac{11\zeta(3)}{6} - \epsilon^4 \frac{101\pi^4}{480} + \mathcal{O}(\epsilon^5). \quad (17)$$

The loop integrals in the planar family do not have a branch cut at  $m_W = 0$  ( $z = 0$ ). Thus, the corresponding canonical differential equations should not have a pole at  $z = 0$ . This regularity condition provides useful information about the boundaries. As can be seen from Eq.(9), the coefficient of  $1/z$  should vanish at  $z = 0$ , which means  $F_2|_{z=0} = 0$ . Due to the same reason, the bases  $F_9$  and  $F_{12}$  are also vanishing at  $z = 0$ , and

$$F_{11}|_{z=0} = \left( F_1 - \frac{F_4}{2} \right) \Big|_{z=0}. \quad (18)$$

The boundary condition for  $F_3$  at  $z = 0$  is calculated directly,

$$F_3|_{z=0} = 1 + \epsilon^2 \frac{\pi^2}{2} - \epsilon^3 \frac{8\zeta(3)}{3} + \epsilon^4 \frac{7\pi^4}{40} + \mathcal{O}(\epsilon^5). \quad (19)$$

In the bases  $\{F_4, F_{23}\}$ , the final-state  $W$  boson and top quark can be considered as a single particle. All the propagators are massless. They appear in the massless double box diagrams. Here we derive independently their values at  $s = m_t^2$ , which can be used as the boundary at  $z = 0, x = 1$ .

$$\begin{aligned} F_4|_{s=m_t^2} &= -1 - 2\epsilon i\pi + \epsilon^2 \frac{13\pi^2}{6} + \epsilon^3 \frac{32\zeta(3) + 5i\pi^3}{3} + \epsilon^4 \left( -\frac{101\pi^4}{120} + \frac{64i\pi\zeta(3)}{3} \right) + \mathcal{O}(\epsilon^5), \\ F_{23}|_{s=m_t^2} &= \frac{1}{4} + \epsilon \frac{i\pi}{2} - \epsilon^2 \frac{11\pi^2}{24} - \epsilon^3 \left( \frac{13\zeta(3)}{6} + \frac{i\pi^3}{4} \right) + \epsilon^4 \left( \frac{79\pi^4}{1440} - \frac{13i\pi\zeta(3)}{3} \right) + \mathcal{O}(\epsilon^5). \end{aligned}$$

The bases  $\{F_6, F_{13}\}$  factorize to a product of two one-loop integrals, and can be computed easily,

$$\begin{aligned} F_6|_{s=m_t^2} &= 1 + \epsilon i\pi - \epsilon^2 \frac{\pi^2}{2} - \epsilon^3 \frac{16\zeta(3) + i\pi^3}{3} + \epsilon^4 \left( \frac{\pi^4}{120} - \frac{8i\pi\zeta(3)}{3} \right) + \mathcal{O}(\epsilon^5), \\ F_{13}|_{s=m_t^2} &= 1 + 2\epsilon i\pi - \epsilon^2 \frac{13\pi^2}{6} - \epsilon^3 \frac{14\zeta(3) + 5i\pi^3}{3} + \epsilon^4 \left( \frac{113\pi^4}{120} - \frac{28i\pi\zeta(3)}{3} \right) + \mathcal{O}(\epsilon^5). \end{aligned}$$

The integrals of  $\{F_5, F_7, F_8, F_{10}, F_{14}, F_{15}, F_{24}, F_{30}\}$  are multiplied by  $r_1$  in the bases, and thus they are vanishing at  $x = 1$ .

The bases  $\{F_{16}, F_{17}\}$  are the same as  $\{F_2, F_3\}$  after replacing  $t$  by  $m_W^2$ . So their boundaries at  $y = 0$  are known from  $\{F_2, F_3\}$  at  $z = 0$ .

From the definitions of the bases, we know that  $F_{18}, F_{22}, F_{26}, F_{27}$  vanish at  $u = m_t^2$  ( $l_{13} = 0$ ),  $t = m_W^2$  ( $y = z^2$ ),  $u = m_W^2$  ( $l_{14} = 0$ ),  $m_W^2 t - m_t^2(s+t+m_W^2) + m_t^4 = 0$  ( $l_{15} = 0$ ), respectively.

The boundary conditions of  $\{F_{19}, F_{20}, F_{21}, F_{25}, F_{28}, F_{29}, F_{31}\}$  are determined from the regularity conditions at  $ut = m_t^2 m_W^2$  ( $x = -\frac{y}{z}$ ).

With the discussion above, we determine all the boundary conditions for the planar family. As a result, one can obtain the analytic results of the basis from the canonical

differential equations directly. We provide the results of the MIs in electronic form in the ancillary files attached to the arXiv submission of the paper. Below we show the first two terms in the expansion of  $\epsilon$ .

$$\begin{aligned}
F_1 &= -\frac{1}{4} + \epsilon \cdot 0 + \mathcal{O}(\epsilon^2), & F_2 &= 0 - \epsilon \cdot \ln(1 - z^2) + \mathcal{O}(\epsilon^2), \\
F_3 &= 1 - \epsilon \cdot 2 \ln(1 - z^2) + \mathcal{O}(\epsilon^2), \\
F_4 &= -1 + \epsilon \cdot 2 \ln\left(\frac{(x+z)(xz+1)}{x}\right) - 2i\pi + \mathcal{O}(\epsilon^2), & F_5 &= 0 - \epsilon \cdot 0 + \mathcal{O}(\epsilon^2), \\
F_6 &= 1 - \epsilon \cdot \ln\left(\frac{(x+z)(xz+1)}{x}\right) + i\pi + \mathcal{O}(\epsilon^2), \\
F_7 &= 0 + \epsilon \cdot 0 + \mathcal{O}(\epsilon^2), & F_8 &= 0 + \epsilon \cdot 0 + \mathcal{O}(\epsilon^2), \\
F_9 &= 0 - \epsilon \cdot \ln(1 - z^2) + \mathcal{O}(\epsilon^2), & F_{10} &= 0 + \epsilon \cdot 0 + \mathcal{O}(\epsilon^2), \\
F_{11} &= \frac{1}{4} + \epsilon \cdot \left[ -\ln\left(\frac{(x+z)(xz+1)}{x}\right) + \ln(1 - z^2) + i\pi \right] + \mathcal{O}(\epsilon^2), \\
F_{12} &= 0 - \epsilon \cdot \ln(1 - z^2) + \mathcal{O}(\epsilon^2), \\
F_{13} &= 1 + \epsilon \cdot \left[ -2 \ln\left(\frac{(x+z)(xz+1)}{x}\right) + 2i\pi \right] + \mathcal{O}(\epsilon^2), & F_{14} &= 0 + \epsilon \cdot 0 + \mathcal{O}(\epsilon^2), \\
F_{15} &= 0 + \epsilon \cdot 0 + \mathcal{O}(\epsilon^2), & F_{16} &= 0 - \epsilon \cdot \ln(1 - y) + \mathcal{O}(\epsilon^2), \\
F_{17} &= 1 - \epsilon \cdot 2 \ln(1 - y) + \mathcal{O}(\epsilon^2), & F_{18} &= 0 + \epsilon \cdot 0 + \mathcal{O}(\epsilon^2), \\
F_{19} &= -\frac{1}{6} + \epsilon \cdot \left[ \frac{1}{2} \ln\left(\frac{(x+z)(xz+1)}{x}\right) - \frac{1}{3} \ln(1 - y) - \frac{i\pi}{2} \right] + \mathcal{O}(\epsilon^2), \\
F_{20} &= 0 - \epsilon \cdot \ln(1 - y) + \mathcal{O}(\epsilon^2), \\
F_{21} &= \frac{5}{8} + \epsilon \cdot \left[ -\frac{1}{2} \ln\left(\frac{(x+z)(xz+1)}{x}\right) - \ln(1 - y) + \frac{1}{2} \ln(1 - z^2) + \frac{i\pi}{2} \right] + \mathcal{O}(\epsilon^2), \\
F_{22} &= 0 + \epsilon \cdot \left[ \frac{1}{2} \ln(1 - y) - \frac{1}{2} \ln(1 - z^2) \right] + \mathcal{O}(\epsilon^2), \\
F_{23} &= \frac{1}{4} + \epsilon \cdot \left[ -\frac{1}{2} \ln\left(\frac{(x+z)(xz+1)}{x}\right) + \frac{i\pi}{2} \right] + \mathcal{O}(\epsilon^2), & F_{24} &= 0 + \epsilon \cdot 0 + \mathcal{O}(\epsilon^2), \\
F_{25} &= \frac{5}{12} + \epsilon \cdot \left[ -\frac{1}{2} \ln\left(\frac{(x+z)(xz+1)}{x}\right) - \frac{7}{6} \ln(1 - y) + \frac{1}{2} \ln(1 - z^2) + \frac{i\pi}{2} \right] + \mathcal{O}(\epsilon^2), \\
F_{26} &= 0 + \epsilon \cdot 0 + \mathcal{O}(\epsilon^2), & F_{27} &= 0 + \epsilon \cdot 0 + \mathcal{O}(\epsilon^2), \\
F_{28} &= 0 + \epsilon \cdot \left[ \frac{1}{2} \ln(1 - y) - \frac{1}{2} \ln(1 - z^2) \right] + \mathcal{O}(\epsilon^2), \\
F_{29} &= -\frac{11}{24} + \epsilon \cdot \left[ \frac{1}{2} \ln\left(\frac{(x+z)(xz+1)}{x}\right) + \frac{4}{3} \ln(1 - y) - \frac{1}{2} \ln(1 - z^2) - \frac{i\pi}{2} \right] + \mathcal{O}(\epsilon^2), \\
F_{30} &= 0 + \epsilon \cdot 0 + \mathcal{O}(\epsilon^2), & F_{31} &= \frac{1}{24} - \epsilon \cdot \frac{1}{6} \ln(1 - y) + \mathcal{O}(\epsilon^2).
\end{aligned} \tag{20}$$

In our calculation, we have varied  $m_W$  in order to choose a proper boundary condition. One may wonder whether the boundary  $m_W = m_t$ , equivalently  $z = 1$ , can be taken. If the answer is yes, then one can make use of all the results of two-loop integrals for  $gg \rightarrow t\bar{t}$ . However, this is non-trivial since  $z = 1$  is the point where a branch cut starts. For example, we can take  $F_1$  as a boundary for  $F_2$  at  $z = 1$  because they are the same

if setting  $m_W^2 = m_t^2$  in the integrands. But we see from above analytic results expanded in  $\epsilon$  that  $F_2|_{z=1} \neq F_1$ . The reason is that the analytic results are valid only for  $z^2 < 1$ . In the  $z \rightarrow 1$  limit, one can not expand the  $(1-z)^{n\epsilon}$  terms in a series of  $\epsilon$  for the master integrals. Instead, one should now solve the differential equation in Eq.(9) with full  $\epsilon$  dependence,

$$\begin{aligned} F_2 &= c_1(1-z)^{-4\epsilon} - c_2, \\ F_3 &= 2c_1(1-z)^{-4\epsilon} + 2c_2. \end{aligned} \quad (21)$$

Comparing these with the analytic results in Eq.(20), we find

$$c_1 = \frac{1}{4} - \epsilon \ln 2 + \mathcal{O}(\epsilon^2), \quad c_2 = \frac{1}{4} + \mathcal{O}(\epsilon^2). \quad (22)$$

Then taking  $(1-z)^{-4\epsilon} \rightarrow 0$  at  $z = 1$ , we see that  $F_2|_{z=1} = F_1$ . If one uses the boundary values at  $z = 1$  for  $F_2$  and  $F_3$ , which are  $-c_2$  and  $2c_2$ , respectively, one still needs the information of  $c_1$  to obtain the results at general  $z$ . But this information can only be obtained at a point other than  $z = 1$ .

All the analytic results are real in the Euclidean regions ( $s < 0, t < 0, u < 0$ ). In this work we are interested in the physical region with  $s > (m_t + m_W)^2, t_0 < t < t_1, 0 < m_W^2 < m_t^2$ ,<sup>1</sup> where

$$\begin{aligned} t_0 &\equiv \frac{m_t^2 + m_W^2 - s - r_1}{2}, \\ t_1 &\equiv \frac{m_t^2 + m_W^2 - s + r_1}{2}. \end{aligned} \quad (23)$$

This region corresponds to  $0 < x < 1, -2z/x < y < -2zx, 0 < z < 1$ . The analytic continuation to this region can be performed by assigning  $s$  a numerically small imaginary part  $i\epsilon$  ( $\epsilon > 0$ ), i.e.,  $s \rightarrow s + i\epsilon$ . This prescription gives the correct numerical results in both the Euclidean and physical regions, when the multiple polylogarithms are evaluated using GiNaC [46, 47].

All the analytical results have been checked with the numerical package FIESTA [48], and they agree within the computation errors in both Euclidean and physical regions. For example, we show the results of two integrals at a physical kinematic point ( $s = 10, t = -2, m_W^2 = \frac{1}{4}, m_t = 1$ ),

$$\begin{aligned} I_{1,0,1,0,1,1,0,0}^{\text{analytic}} &= \frac{0.00475421 + 1.48022009 i}{\epsilon} \\ &+ (-5.24410651 + 1.22399295 i), \end{aligned} \quad (24)$$

$$\begin{aligned} I_{1,0,1,0,1,1,0,0}^{\text{FIESTA}} &= \frac{0.004754 + 1.48022 i \pm 0.000056(1 + i)}{\epsilon} \\ &+ (-5.24410 + 1.22399 i) \pm (0.000416 + 0.000415 i), \end{aligned} \quad (25)$$

and

$$I_{1,1,1,1,1,0,1,0,0}^{\text{analytic}} = \frac{0.0308065}{\epsilon^3} + \frac{-0.06040731}{\epsilon^2} + \frac{0.22341495 - 0.06475586 i}{\epsilon}$$

---

<sup>1</sup>Notice that the physical region with  $0 < s < (m_t - m_W)^2, t_1 < t < t_0, 0 < m_W^2 < m_t^2$  corresponds to top quark decay  $t \rightarrow Wbg$ , and our prescription for the analytic continuation is applicable in this case.

$$\begin{aligned}
& + (-0.26302494 + 0.62749975 i), \\
I_{1,1,1,1,1,0,0,0,0}^{\text{FIESTA}} &= \frac{0.030807 \pm 0.000005}{\epsilon^3} + \frac{-0.060407 \pm 0.000027}{\epsilon^2}
\end{aligned} \tag{26}$$

$$\begin{aligned}
& + \frac{0.223415 - 0.064756 i \pm (0.000116 + 0.000124 i)}{\epsilon} \\
& + (-0.263019 + 0.627484 i) \pm (0.000392 + 0.000395 i).
\end{aligned} \tag{27}$$

## 4 Conclusion

We calculate analytically two-loop master integrals for hadronic  $tW$  productions that contain only one massive propagator. After choosing a canonical basis, the differential equations for the master integrals can be transformed into the  $d \ln$  form. The boundaries are determined by simple direct integrations or regularity conditions at kinematic points without physical singularities. The analytical results in this work are expressed in terms of multiple polylogarithms, and have been checked with numerical computations. There is still a lot of work to do in the future to obtain the complete two-loop virtual corrections in this channel.

## Acknowledgments

This work was supported in part by the National Natural Science Foundation of China under Grant No. 11805042, 12005117, and 12175048. The work of JW was also supported by Taishan Scholar Foundation of Shandong province (No. tsqn201909011).

## Appendix: Results of the non-planar integral family

For the master integral shown in Fig.2(b), we define the non-planar integral family by

$$J_{n_1, n_2, \dots, n_9} = \int \mathcal{D}^D q_1 \mathcal{D}^D q_2 \frac{1}{P_1^{n_1} P_2^{n_2} P_3^{n_3} P_4^{n_4} P_5^{n_5} P_6^{n_6} P_7^{n_7} P_8^{n_8} P_9^{n_9}} \tag{28}$$

with the denominators

$$\begin{aligned}
P_1 &= q_1^2, & P_2 &= (q_1 - q_2)^2, & P_3 &= q_2^2, & P_4 &= (q_1 + k_1)^2, \\
P_5 &= (q_1 - q_2 - k_2)^2, & P_6 &= (q_2 + k_1 + k_2)^2, & P_7 &= (q_2 + k_1 + k_2 - k_3)^2 - m_t^2, \\
P_8 &= (q_1 - k_3)^2, & P_9 &= (q_2 + k_1)^2.
\end{aligned}$$

The canonical bases are chosen to be

$$\begin{aligned}
B_1 &= m_t^2 N_1, & B_2 &= m_W^2 N_2, & B_3 &= (m_W^2 - m_t^2) N_3 - 2m_t^2 N_2, \\
B_4 &= (-s) N_4, & B_5 &= r_1 N_5, & B_6 &= (m_W^2 + m_t^2 - s - t) N_6, \\
B_7 &= (m_W^2 - s - t) N_7 - 2m_t^2 N_6, & B_8 &= (m_W^2 - s - t) N_8, \\
B_9 &= s N_9, & B_{10} &= t N_{10}, & B_{11} &= (t - m_t^2) N_{11} - 2m_t^2 N_{10},
\end{aligned}$$

$$\begin{aligned}
B_{12} &= (t - m_W^2) N_{12}, \quad B_{13} = r_1 N_{13}, \\
B_{14} &= m_t^2(-s) N_{14} - \frac{3}{2}(m_t^2 - m_W^2 + s) N_{13}, \\
B_{15} &= r_1 N_{15}, \quad B_{16} = s(s + t - m_W^2) N_{16}, \quad B_{17} = (t - m_t^2) N_{17}, \\
B_{18} &= m_t^2(-s) N_{18}, \quad B_{19} = r_1 N_{19}, \quad B_{20} = (t - m_t^2)(-s) N_{20}, \\
B_{21} &= (m_W^2 - s - t) N_{21}, \quad B_{22} = m_t^2(-s) N_{22}, \quad B_{23} = (m_t^2 - s - t) N_{23}, \\
B_{24} &= -(t m_W^2 - (m_W^2 + s + t) m_t^2 + m_t^4) N_{24}, \quad B_{25} = (t - m_W^2) N_{25}, \\
B_{26} &= (m_W^2(s + t - m_W^2) - m_t^2(t - m_W^2)) N_{26}, \quad B_{27} = (-s) N_{27}, \\
B_{28} &= (t - m_t^2)(m_W^2 - s - t) N_{28}, \quad B_{29} = (m_W^2 - m_t^2)s N_{29}, \\
B_{30} &= (t - m_W^2) N_{30} + (m_W^2 - s - t) N_{27}, \quad B_{31} = s^2 N_{31}, \\
B_{32} &= (s + t - m_W^2) \left( s^2 N_{32} + s N_{33} - s N_{29} + \frac{1}{4}(s + t - m_t^2) N_{28} + \frac{N_{11}}{8} \right) \\
&+ \frac{(s + t - m_W^2)}{(t - m_t^2)} \left( \frac{3}{2} N_{21} (-m_W^2 + s + t) + N_{22} s m_t^2 + \frac{1}{4} N_2 (m_t^2 + 2m_W^2) \right. \\
&+ \frac{1}{8} N_3 (m_t^2 - m_W^2) - \frac{1}{4} N_{10} (m_t^2 + 2t) - \frac{3N_4 s}{8} \Big) \\
&+ \frac{1}{4\epsilon + 1} \left[ -\frac{1}{8} (2N_{28}s + N_7 + N_{11}) (-m_W^2 + s + t) + N_{18} s m_t^2 \right. \\
&+ \frac{1}{4} N_6 [2(-m_W^2 + s + t) - 3m_t^2] + \frac{3}{2} N_{17} (m_t^2 - t) \\
&+ \frac{s + t - m_W^2}{t - m_t^2} \left( -\frac{3}{2} N_{21} (-m_W^2 + s + t) + N_{22}(-s)m_t^2 + \frac{1}{4} N_{10} (m_t^2 + 2t) \right) \\
&+ \left. \frac{s + m_t^2 - m_W^2}{t - m_t^2} \left( -\frac{1}{4} N_2 (m_t^2 + 2m_W^2) + \frac{1}{8} N_3 (m_W^2 - m_t^2) + \frac{3N_4 s}{8} \right) \right] \\
B_{33} &= (t - m_t^2)(-s) N_{33}, \\
B_{34} &= r_1 \left[ N_{34} + s N_{33} - N_{30} - \frac{1}{4}(s + t - m_W^2) N_{28} + \frac{1}{2} N_{17} - \frac{1}{12} N_{11} \right. \\
&+ \frac{1}{t - m_t^2} \left( \frac{m_t^2}{4} N_1 - \frac{m_t^2 + 2m_W^2}{4} N_2 - \frac{m_t^2 - m_W^2}{8} N_3 \right. \\
&+ \left. \left. \frac{3s}{8} N_4 + \frac{2t + m_t^2}{6} N_{10} - \frac{3}{2}(s + t - m_W^2) N_{21} - m_t^2 s N_{22} \right) \right]. \tag{29}
\end{aligned}$$

with

$$\begin{aligned}
N_1 &= \epsilon^2 J_{1,2,0,0,0,0,2,0,0}, & N_2 &= \epsilon^2 J_{0,0,0,1,2,0,2,0,0}, & N_3 &= \epsilon^2 J_{0,0,0,2,2,0,1,0,0}, \\
N_4 &= \epsilon^2 J_{0,0,1,2,2,0,0,0,0}, & N_5 &= \epsilon^3 J_{0,0,1,1,2,0,1,0,0}, & N_6 &= \epsilon^2 J_{0,1,0,2,0,0,2,0,0}, \\
N_7 &= \epsilon^2 J_{0,2,0,2,0,0,1,0,0}, & N_8 &= \epsilon^3 J_{0,1,0,2,0,1,1,0,0}, & N_9 &= \epsilon^3 J_{0,1,1,2,0,1,0,0,0}, \\
N_{10} &= \epsilon^2 J_{1,0,0,0,2,0,2,0,0}, & N_{11} &= \epsilon^2 J_{2,0,0,0,2,0,1,0,0}, & N_{12} &= \epsilon^3 J_{1,0,0,0,2,1,1,0,0}, \\
N_{13} &= \epsilon^3 J_{1,2,0,0,0,1,1,0,0}, & N_{14} &= \epsilon^2 J_{1,2,0,0,0,1,2,0,0}, & N_{15} &= \epsilon^3 (1 - 2\epsilon) J_{0,1,1,1,0,1,1,0,0}, \\
N_{16} &= \epsilon^3 J_{0,1,1,2,0,1,1,0,0}, & N_{17} &= \epsilon^4 J_{0,1,1,1,1,0,1,0,0}, & N_{18} &= \epsilon^3 J_{0,1,1,1,1,0,2,0,0}, \\
N_{19} &= \epsilon^3 (1 - 2\epsilon) J_{1,0,1,0,1,1,1,0,0}, & N_{20} &= \epsilon^3 J_{1,0,1,0,2,1,1,0,0}, & N_{21} &= \epsilon^4 J_{1,0,1,1,1,0,1,0,0}, \\
N_{22} &= \epsilon^3 J_{1,0,1,1,1,0,2,0,0}, & N_{23} &= \epsilon^4 J_{1,1,0,0,1,1,1,0,0}, & N_{24} &= \epsilon^3 J_{1,1,0,0,1,1,2,0,0}, \\
N_{25} &= \epsilon^4 J_{1,1,0,1,0,1,1,0,0}, & N_{26} &= \epsilon^3 J_{1,1,0,1,0,1,2,0,0}, & N_{27} &= \epsilon^4 J_{1,1,0,1,1,0,1,0,0}, \\
N_{28} &= \epsilon^3 J_{1,1,0,1,1,0,2,0,0}, & N_{29} &= \epsilon^4 J_{1,1,0,1,1,1,1,0,0}, & N_{30} &= \epsilon^4 J_{1,1,0,1,1,1,1,0,-1},
\end{aligned}$$

$$\begin{aligned}
N_{31} &= \epsilon^4 J_{1,1,1,1,1,1,0,0,0}, & N_{32} &= \epsilon^4 J_{1,1,1,1,1,1,1,0,0}, \\
N_{33} &= \epsilon^4 J_{1,1,1,1,1,1,0,0,-1}, & N_{34} &= \epsilon^4 J_{1,1,1,1,1,1,1,0,-2}.
\end{aligned} \tag{30}$$

The canonical differential equations for  $\mathbf{B} = (B_1, \dots, B_{34})$  can be written as

$$d\mathbf{B}(x, y, z; \epsilon) = \epsilon (d\tilde{C}) \mathbf{B}(x, y, z; \epsilon), \tag{31}$$

with

$$d\tilde{C} = \sum_{i=1}^{17} Q_i d\ln(l_i), \tag{32}$$

where  $Q_i$  are rational matrices.

The non-planar and planar diagrams share some common integrals. For the non-planar family, we find that

$$\begin{aligned}
B_1 &= F_1, & B_2 &= F_2, & B_3 &= F_3, & B_4 &= F_4, \\
B_5 &= F_5, & B_9 &= -F_{23}, & B_{10} &= F_{16}, & B_{11} &= F_{17}, \\
B_{12} &= F_{22}, & B_{13} &= F_{10}, & B_{14} &= F_{11}, & B_{19} &= F_{24}, \\
B_{20} &= F_{25}, & B_{23} &= F_{26}, & B_{24} &= F_{27}.
\end{aligned} \tag{33}$$

For the other unknown integrals in the non-planar family, their boundary conditions are obtained as follows. The base  $B_6$  is vanishing at  $u = 0$  ( $l_{16} = 0$ ), and the boundary conditions for  $B_7$  at  $u = 0$  are equal to  $B_3$  at  $m_W = 0$ . The base  $B_8$  vanishes at  $u = m_W^2$ . The bases  $\{B_{15}, B_{34}\}$  vanish at  $s = (m_t + m_W)^2$ . The base  $B_{17}$  is vanishing at  $t = m_t^2$ . The base  $B_{21}$  equals to zero at  $u = m_t^2$ . The base  $B_{27}$  is vanishing at  $s = 0$ . The base  $B_{30}$  is zero at  $u = m_W^2$ . The base  $B_{26}$  equals to zero at  $m_W^2(s + t - m_W^2) - m_t^2(t - m_W^2) = 0$ , i.e.  $l_{17} = 0$ . The result of  $B_{31}$  can be found in Ref.[49]. The boundary conditions for bases  $\{B_{16}, B_{18}, B_{22}, B_{25}, B_{28}, B_{29}, B_{32}, B_{33}\}$  are determined from the regularity conditions at  $u t = m_t^2 m_W^2$ . The analytical results are expressed in terms of multiple polylogarithms. We provide them in the ancillary file, which can be evaluated using **GiNaC**. In the physical region, one needs to assign  $s$  and  $t$  a numerically small but positive imaginary part.

## References

- [1] ATLAS collaboration, G. Aad et al., *Evidence for the associated production of a  $W$  boson and a top quark in ATLAS at  $\sqrt{s} = 7$  TeV*, *Phys. Lett.* **B716** (2012) 142–159, [1205.5764].
- [2] ATLAS collaboration, G. Aad et al., *Measurement of the production cross-section of a single top quark in association with a  $W$  boson at 8 TeV with the ATLAS experiment*, *JHEP* **01** (2016) 064, [1510.03752].
- [3] ATLAS collaboration, M. Aaboud et al., *Measurement of the cross-section for producing a  $W$  boson in association with a single top quark in  $pp$  collisions at  $\sqrt{s} = 13$  TeV with ATLAS*, *JHEP* **01** (2018) 063, [1612.07231].

- [4] ATLAS collaboration, M. Aaboud et al., *Measurement of differential cross-sections of a single top quark produced in association with a  $W$  boson at  $\sqrt{s} = 13$  TeV with ATLAS*, *Eur. Phys. J.* **C78** (2018) 186, [1712.01602].
- [5] CMS collaboration, S. Chatrchyan et al., *Evidence for associated production of a single top quark and  $W$  boson in  $pp$  collisions at  $\sqrt{s} = 7$  TeV*, *Phys. Rev. Lett.* **110** (2013) 022003, [1209.3489].
- [6] CMS collaboration, S. Chatrchyan et al., *Observation of the associated production of a single top quark and a  $W$  boson in  $pp$  collisions at  $\sqrt{s} = 8$  TeV*, *Phys. Rev. Lett.* **112** (2014) 231802, [1401.2942].
- [7] CMS collaboration, A. M. Sirunyan et al., *Measurement of the production cross section for single top quarks in association with  $W$  bosons in proton-proton collisions at  $\sqrt{s} = 13$  TeV*, *JHEP* **10** (2018) 117, [1805.07399].
- [8] W. T. Giele, S. Keller and E. Laenen,  *$QCD$  corrections to  $W$  boson plus heavy quark production at the Tevatron*, *Phys. Lett.* **B372** (1996) 141–149, [hep-ph/9511449].
- [9] S. Zhu, *Next-to-leading order  $QCD$  corrections to  $bg \rightarrow tW^-$  at CERN large hadron collider*, *Phys. Lett.* **B524** (2002) 283–288, [hep-ph/0109269].
- [10] Q.-H. Cao, *Demonstration of One Cutoff Phase Space Slicing Method: Next-to-Leading Order  $QCD$  Corrections to the  $tW$  Associated Production in Hadron Collision*, 0801.1539.
- [11] P. Kant, O. M. Kind, T. Kintscher, T. Lohse, T. Martini, S. Mölbitz et al., *HatHor for single top-quark production: Updated predictions and uncertainty estimates for single top-quark production in hadronic collisions*, *Comput. Phys. Commun.* **191** (2015) 74–89, [1406.4403].
- [12] J. M. Campbell and F. Tramontano, *Next-to-leading order corrections to  $Wt$  production and decay*, *Nucl. Phys.* **B726** (2005) 109–130, [hep-ph/0506289].
- [13] S. Frixione, E. Laenen, P. Motylinski, B. R. Webber and C. D. White, *Single-top hadroproduction in association with a  $W$  boson*, *JHEP* **07** (2008) 029, [0805.3067].
- [14] E. Re, *Single-top  $Wt$ -channel production matched with parton showers using the POWHEG method*, *Eur. Phys. J.* **C71** (2011) 1547, [1009.2450].
- [15] T. Ježo, J. M. Lindert, P. Nason, C. Oleari and S. Pozzorini, *An  $NLO+PS$  generator for  $t\bar{t}$  and  $Wt$  production and decay including non-resonant and interference effects*, *Eur. Phys. J.* **C76** (2016) 691, [1607.04538].
- [16] C. S. Li, H. T. Li, D. Y. Shao and J. Wang, *Momentum-space threshold resummation in  $tW$  production at the LHC*, *JHEP* **06** (2019) 125, [1903.01646].
- [17] N. Kidonakis, *Single top production at the Tevatron: Threshold resummation and finite-order soft gluon corrections*, *Phys. Rev.* **D74** (2006) 114012, [hep-ph/0609287].
- [18] N. Kidonakis, *Two-loop soft anomalous dimensions for single top quark associated production with a  $W^-$  or  $H^-$* , *Phys. Rev.* **D82** (2010) 054018, [1005.4451].

- [19] N. Kidonakis, *Soft-gluon corrections for  $tW$  production at  $N^3LO$* , *Phys. Rev.* **D96** (2017) 034014, [1612.06426].
- [20] N. Kidonakis and N. Yamanaka, *Higher-order corrections for  $tW$  production at high-energy hadron colliders*, *JHEP* **05** (2021) 278, [2102.11300].
- [21] T. M. P. Tait, *The  $tW^-$  mode of single top production*, *Phys. Rev.* **D61** (1999) 034001, [hep-ph/9909352].
- [22] A. S. Belyaev, E. E. Boos and L. V. Dudko, *Single top quark at future hadron colliders: Complete signal and background study*, *Phys. Rev. D* **59** (1999) 075001, [hep-ph/9806332].
- [23] A. Belyaev and E. Boos, *Single top quark  $tW + X$  production at the CERN LHC: A Closer look*, *Phys. Rev.* **D63** (2001) 034012, [hep-ph/0003260].
- [24] C. D. White, S. Frixione, E. Laenen and F. Maltoni, *Isolating  $Wt$  production at the LHC*, *JHEP* **11** (2009) 074, [0908.0631].
- [25] F. Demartin, B. Maier, F. Maltoni, K. Mawatari and M. Zaro,  *$tWH$  associated production at the LHC*, *Eur. Phys. J.* **C77** (2017) 34, [1607.05862].
- [26] H. T. Li and J. Wang, *Next-to-Next-to-Leading Order  $N$ -Jettiness Soft Function for One Massive Colored Particle Production at Hadron Colliders*, *JHEP* **02** (2017) 002, [1611.02749].
- [27] H. T. Li and J. Wang, *Next-to-next-to-leading order  $N$ -jettiness soft function for  $tW$  production*, *Phys. Lett.* **B784** (2018) 397–404, [1804.06358].
- [28] K. G. Chetyrkin and F. V. Tkachov, *Integration by Parts: The Algorithm to Calculate beta Functions in 4 Loops*, *Nucl. Phys. B* **192** (1981) 159–204.
- [29] A. V. Smirnov and A. V. Petukhov, *The Number of Master Integrals is Finite*, *Lett. Math. Phys.* **97** (2011) 37–44, [1004.4199].
- [30] C. Anastasiou and A. Lazopoulos, *Automatic integral reduction for higher order perturbative calculations*, *JHEP* **07** (2004) 046, [hep-ph/0404258].
- [31] A. von Manteuffel and C. Studerus, *Reduze 2 - Distributed Feynman Integral Reduction*, 1201.4330.
- [32] R. N. Lee, *Presenting LiteRed: a tool for the Loop InTEgrals REDuction*, 1212.2685.
- [33] A. V. Smirnov and F. S. Chuharev, *FIRE6: Feynman Integral REDuction with Modular Arithmetic*, *Comput. Phys. Commun.* **247** (2020) 106877, [1901.07808].
- [34] J. Klappert, F. Lange, P. Maierhöfer and J. Usovitsch, *Integral Reduction with Kira 2.0 and Finite Field Methods*, 2008.06494.
- [35] S. Laporta, *High precision calculation of multiloop Feynman integrals by difference equations*, *Int. J. Mod. Phys. A* **15** (2000) 5087–5159, [hep-ph/0102033].
- [36] G. Heinrich, *Collider Physics at the Precision Frontier*, 2009.00516.

- [37] J. Blümlein, *Analytic integration methods in quantum field theory: an Introduction*, 2103.10652.
- [38] A. V. Kotikov, *Differential equations method: New technique for massive Feynman diagrams calculation*, *Phys. Lett.* **B254** (1991) 158–164.
- [39] A. V. Kotikov, *Differential equation method: The Calculation of  $N$  point Feynman diagrams*, *Phys. Lett.* **B267** (1991) 123–127.
- [40] J. M. Henn, *Multiloop integrals in dimensional regularization made simple*, *Phys. Rev. Lett.* **110** (2013) 251601, [1304.1806].
- [41] N. u. Basat, Z. Li and Y. Wang, *Reduction of planar double-box diagram for single-top production via auxiliary mass flow*, 2102.08225.
- [42] S. Di Vita, T. Gehrmann, S. Laporta, P. Mastrolia, A. Primo and U. Schubert, *Master integrals for the NNLO virtual corrections to  $q\bar{q} \rightarrow t\bar{t}$  scattering in QCD: the non-planar graphs*, *JHEP* **06** (2019) 117, [1904.10964].
- [43] M. Argeri, S. Di Vita, P. Mastrolia, E. Mirabella, J. Schlenk, U. Schubert et al., *Magnus and Dyson Series for Master Integrals*, *JHEP* **03** (2014) 082, [1401.2979].
- [44] A. B. Goncharov, *Multiple polylogarithms, cyclotomy and modular complexes*, *Math. Res. Lett.* **5** (1998) 497–516, [1105.2076].
- [45] L.-B. Chen, Y. Liang and C.-F. Qiao, *Two-Loop integrals for CP-even heavy quarkonium production and decays*, *JHEP* **06** (2017) 025, [1703.03929].
- [46] J. Vollinga and S. Weinzierl, *Numerical evaluation of multiple polylogarithms*, *Comput. Phys. Commun.* **167** (2005) 177, [hep-ph/0410259].
- [47] C. W. Bauer, A. Frink and R. Kreckel, *Introduction to the GiNaC framework for symbolic computation within the C++ programming language*, *J. Symb. Comput.* **33** (2000) 1, [cs/0004015].
- [48] A. V. Smirnov, *FIESTA4: Optimized Feynman integral calculations with GPU support*, *Comput. Phys. Commun.* **204** (2016) 189–199, [1511.03614].
- [49] R. J. Gonsalves, *DIMENSIONALLY REGULARIZED TWO LOOP ON-SHELL QUARK FORM-FACTOR*, *Phys. Rev. D* **28** (1983) 1542.